CARBON ISOTOPE FRACTIONATION BY CYANOBACTERIA UNDER LIGHT-LIMITING CONDITIONS

By
Kunmanee Bubphamanee
Department of Geological Sciences,
University of Colorado at Boulder

Defense Date: April 5, 2019

Thesis Advisor:
Prof. Boswell Wing, Department of Geological Sciences
Dr. Sarah Hurley, Department of Geological Sciences

Defense Committee:
Prof. Boswell Wing, Department of Geological Sciences
Prof. Charles Stern, Department of Geological Sciences
Prof. Jeffrey Cameron, Department of Biochemistry
Dr. Sarah Hurley, Department of Geological Sciences

Abstract

The evolution of oxygenic photosynthesis and the resulting accumulation of oxygen in the atmosphere, known as the Great Oxidation Event (GOE), is one of the most prominent transitions in Earth history. While cyanobacteria are thought to be responsible for the accumulation of oxygen during the GOE, the timing of the evolution of oxygenic photosynthesis, and the abundance of different primary producers during this time remains unconstrained. The carbon isotopes provide a continuous record through this time period and may be a way to investigate the dominant primary producers during this time. In order to interpret the geologic carbon isotope record, or the offset between preserved carbonate rocks and synchronous organic carbon (ε_{TOC}), we need to understand the underlying carbon isotope fractionation by primary producers (ε_P). Here we investigate the influence of CO_2 concentration and the growth rate on carbon isotope fractionation by four cyanobacterial strains. Under light-limiting conditions, we find a single relationship between ε_P values and growth rate across all strains. Our results suggest that carbon isotope fractionation by cyanobacteria is not strain-specific, but is instead controlled by underlying physiology. These results support the use ε_P values as a proxy for unicellular cyanobacteria. Further work is necessary to understand the factors influencing ε_P values in different conditions and to understand how ε_P values relate to the geologic carbon isotope record.

Acknowledgement

I would like to express my special thank and gratitude to my advisor, Professor Boswell Wing for his enthusiasm and for introducing me into the field of geobiology research. I would like to extend my thanks to my second advisor, Dr. Sarah Hurley, for providing opportunity and giving valuable guidance that helped me through the process of research and writing of this thesis. Without their guidance, it would not be possible to conduct this successful research. Besides my advisors, I want to thank my thesis committee: Professor Jeffrey Cameron for offering me the resource in running the experiment in the Cameron Laboratory, and Professor Charles Stern for insightful comments and suggestions. I thank Brett Davidheiser and Evan Johnson for all of the assistance in the lab. I want to extend my gratitude to the Biological Science Initiative (BSI) for the funding throughout the experiment and providing opportunity in a diverse perspective of science. And finally, I want to thank my family and friends, especially Kasdi Sujono, for all support and encouragement throughout my study.

Table of Contents

1. Introduction

Surface environments have changed dramatically over the course of Earth's history. Over the past 4.6 billion years, Earth's atmosphere has become more oxygenated, while CO_2 levels have decreased through time (Figure 1.1) (Lyons et al., 2014). The atmosphere during the Archaean Eon (4 – 2.5 billion years ago) was thought to be anoxic with abundant of carbon dioxide and methane (Nisbet and Fowler, 2011). Estimates suggest that Archean CO_2 levels were ~10-100 times higher than the present atmospheric levels (PAL) (Kaufman and Xiao, 2003; Crockford et al., 2019). The Archaean oceans were similarly anoxic and contained high concentrations of dissolved iron (Knoll Andrew H. et al., 2016). During Earth's middle age, the Proterozoic (2.5-0.5 billion years ago), atmospheric oxygen levels increased to 10^{-4}-10^{-2} PAL with CO_2 estimates ranging from 10-100 PAL (Kaufman and Xiao, 2003). The oceans became at least partially oxygenated and oxygen eventually surpassed ferrous iron as the dominant electron donor (Knoll Andrew H. et al., 2016). The oxygenation of the oceans in turn led to an expansion of aerobic metabolisms and dramatically increased the magnitude of primary production (Canfield, 2004). The co-evolution of Earth's surface environments and the biosphere led to the Cambrian explosion, at the beginning of Phanerozoic (0.5 billion years to present day), in which major animals and plants appeared in the geologic record and the environment closely resembled the present day landscape.

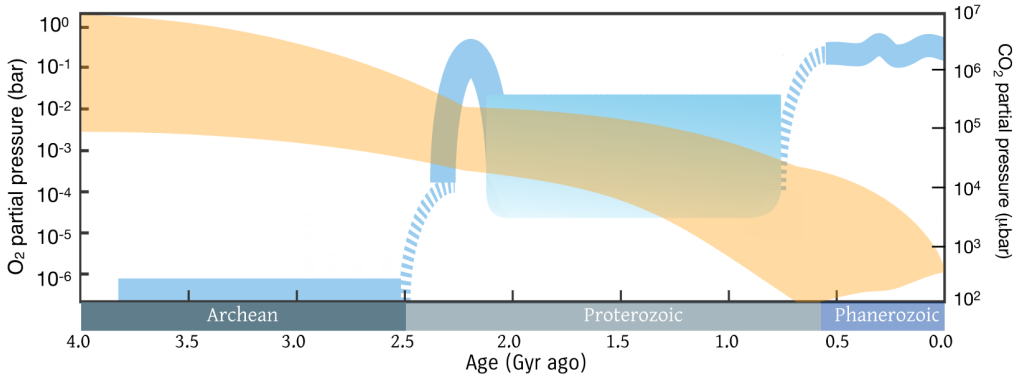

Figure 1.1: The evolution of atmospheric oxygen and carbon dioxide concentrations over Earth history. The blue curve shows the atmospheric oxygen partial pressure (Lyons et al., 2014) and the orange curve shows the atmospheric carbon dioxide partial pressure (Kaufman and Xiao, 2003).

1.1 The evolution of oxygenic photosynthesis

The Great Oxidation Event (GOE), which occurred between 2.3 to 2.4 billion years ago, is one of the most prominent transitions in Earth history. The evolution of oxygenic photosynthesis is thought to be responsible for this rise of free oxygen in the atmosphere. The GOE changed the chemistry of the Earth's atmosphere and oceans, creating oxic environments. The presence of sedimentary iron formations indicates the accumulation of oxygen in the atmosphere (Lyons et al., 2014). Moreover, some Archean successions contain elevated levels of oxygen-mobilized trace elements (Planavsky et al., 2014). Even though the Archaean evidence is limited due to Earth's plate tectonics, the consistent isotopic records suggest the presence of biological carbon and sulfur cycles (Knoll Andrew H. et al., 2016).

Oxygenic photosynthesis evolved in the ancestors of cyanobacteria, although the timing of this metabolism emergence remains unresolved (Shih et al., 2017). Cyanobacteria are thought to be responsible for the accumulation of oxygen during Paleoproterozoic due to the absence of the alternate sources of abundant free oxygen (Bekker et al., 2004; Rasmussen et al., 2013; Ward et al., 2016). The timing of the GOE thus provides a minimum age for the cyanobacterial ancestor. Meanwhile, the first fossils widely cited as photosynthetic eukaryotes appear in ~1.1-1.2 Ga rocks (Butterfield et al., 1990). Eukaryotic photoautotrophs acquired photosynthesis via an endosymbiotic event involving engulfment of an ancestral cyanobacterium (Martin and Kowallik, 1999); therefore, the timing of this event could signal an ecological shift in primary producers. Molecular clock analyses give a broad range of estimates for this primary plastid endosymbiosis from ~0.8 Ga to ~1.7 Ga (Yoon et al., 2004; Douzery et al., 2004; Parfrey et al., 2011; Shih and Matzke, 2013; Shih et al., 2017). As inferred from stromatolite textures, preserved organic biomarkers, and the morphology and environmental distribution of preserved microfossils (e.g. Knoll et al., 2016), these relationships suggest that cyanobacteria may have been the ecologically dominant oxygenic primary producers on Earth for at least ~1 billion years.

While the GOE was one of the most major transitions in Earth history the timing of the evolution of oxygenic photosynthesis remains uncertain. Moreover, the transition to cyanobacteria as the dominant primary producers in relation to the GOE is still in

question. Cyanobacterial fossils are hard to distinguish from inorganic mineral grains and are microscopic size. We therefore need alternate ways to investigate the ancient biosphere. The carbon isotope composition of ancient biosynthetic products could reveal the co-evolution of cyanobacteria and the atmosphere.

1.2 The carbon isotope record

The carbon isotopic difference between carbonates rocks and preserved organic carbon provides a record of carbon fixation by primary producers through Earth history. The carbon isotope composition of organic carbon preserved in sedimentary rocks reflects the isotope composition of biomass produced via primary productivity (Figure 1.2). The carbon isotope composition of carbonate minerals reflects the isotopic composition of inorganic carbon, or the substrate for carbon fixation by primary producers (Figure 1.2). The carbon isotopic difference between preserved organic carbon and carbonate minerals is expressed as ε_{TOC} (Figure 1.3).

(1.1) $$\varepsilon_{TOC} \equiv \delta^{13}C_{CaCO_3} - \delta^{13}C_{TOC}$$

Values of ε_{TOC} preserved in the geologic record can be related to the carbon isotope fractionation associated with carbon fixation in primary productivity (ε_P) through the following equation (Figure 1.3):

(1.2) $$\varepsilon_{TOC} = \varepsilon_p + \Delta_{carb} - \Delta_2$$

Here, Δ_{carb} and Δ_2 represent isotopic fractionations that occur as the primary inorganic substrates and organic products of carbon fixation are preserved in the geologic record, respectively. The isotopic difference between dissolved CO_2 and primary biomass represents the fractionation associated with primary productivity (ε_P):

(1.3) $$\varepsilon_P = \delta^{13}C_{CO_2} - \delta^{13}C_{Biomass}$$

The direct relationship between ε_{TOC} and ε_P suggests that carbon isotopes provide a

record of primary producers through Earth history. This application, however, requires 1) characterizing carbon isotope fractionation by different primary producers, such as cyanobacteria, and 2) understanding how physiology and environmental changes affect this signal. Here we characterize carbon isotope fractionation by four strains of cyanobacteria under modern and ancient conditions to understand if ε_P values represent are primarily influences by physiology or environment. If we can understand the controls on ε_P, we can use this proxy to investigate the evolution of oxygenic photosynthesis under different atmospheric conditions from ε_{TOC} values in the sedimentary record.

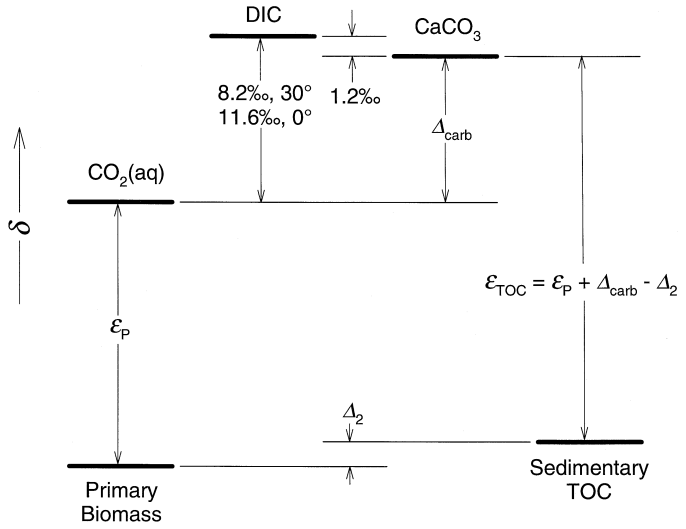

Figure 1.2: Schematic summary of isotopic relationships between ε_P and ε_{TOC} (Hayes et al., 1999)

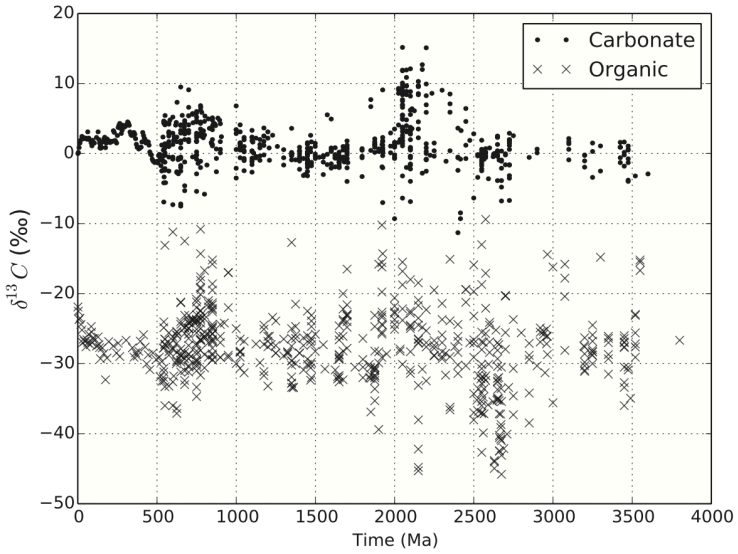

Figure 1.3: The carbonate and organic carbon isotope record throughout Earth's history (Krissansen-Totton et al., 2015).

1.3 Carbon isotope fractionation by cyanobacteria

A phenomenological model based on C3-plants provides an initial framework to predict how environmental and physiological changes may impact carbon isotope fractionation by cyanobacteria (Hayes, 2001). Both cyanobacteria and C3-plants fix CO_2 via the Calvin-Benson-Bassham (CBB) cycle (Badger et al., 2002). The enzyme RubisCO involved in the Calvin cycle fixes CO_2. The phenomenological model includes two processes: the transport of inorganic C (C_i) into the cell and fixation of dissolved CO_2 inside the cell. The isotope effect associated with primary productivity or photoautotrophic carbon fixation (ε_P) can be expressed as follows:

(1.4) $$\varepsilon_P = \varepsilon_f - f(\varepsilon_f - \varepsilon_t)$$

Here ε_t is the isotope effect associated with transport of CO_2 from the external environment to the site of carbon fixation, ε_f is the isotope effect associated with enzymatic conversion of inorganic carbon into a fixed form, and f represents the proportion of carbon that is fixed versus removed from the site of carbon fixation.

The kinetic isotope effect associated with ribulose-1,5-bisphosphate

carboxylase/oxygenase (RuBisCO), the rate-limiting enzyme in carbon fixation via the Calvin-Benson-Bassham cycle, sets an approximate upper bound for ε_P via ε_f . Extant cyanobacteria fix C primarily using Form 1B RuBisCO, which has a kinetic isotope effect of ~22‰ (Guy et al., 1993). The full expression of this isotope effect is attenuated as a greater fraction of the carbon flow to RuBisCO is fixed (as f increases). In algae, physiological controls of the magnitude of relative carbon flow through this branch point have been investigated intensively and include the concentration of $CO_{2(aq)}$, growth rate, and the ratio of cellular volume to surface area (Goericke et al., 1994; Laws et al., 1995; Bidigare et al., 1997; Laws et al., 1997; Rau et al., 1997; Popp et al., 1998).

While the phenomenological model provides a useful framework suggesting that CO_2 concentration and growth rate may affect ε_P values in cyanobacteria, it does not fully capture the processes involved in carbon fixation by modern carbon fixation. All modern cyanobacteria have a carbon concentrating mechanism or CCM (Price and Badger, 2003; Rae et al., 2013). Cyanobacterial CCMs consist of two parts: C_i uptake system and carboxysome. A carboxysome is a protein microcompartment within the cell that contains a carbonic anhydrase (CA) and enzyme ribulose 1,5-biphosphate carboxylase/oxygenase (RubisCO). The CA enzyme converts accumulated HCO_3^- into CO_2, which elevates the interior CO_2 concentrations, allowing RuBisCO carboxylation to outcompete oxygenation. The timing of the emergence of cyanobacterial CCM remains uncertain, however some have suggested it was later (2.4-0.4 billion years ago) because higher CO_2 estimates for the Proterozoic suggest a CCM might not have been necessary (Price and Badger, 2003).

Here we test the validity of this phenomenological model by characterizing cyanobacterial ε_P values across different strains, CO_2 concentrations, and growth rates.

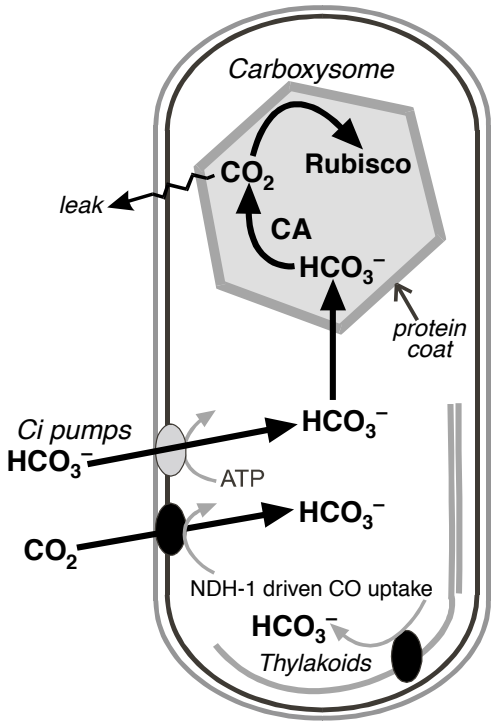

Figure 1.4: A model of a cyanobacterial cell with components of the CO_2-concentration mechanism shown on the figure are the Rubisco containing carboxysome, with carbonic anhydrase (CA) and an associated diffusional resistance to CO_2 efflux, the accumulation of HCO_3^- in the cytosol, and a number of CO_2 and HCO_3^- transport systems located both on the plasma membrane and the thylakoid (Badger et al., 2002).

1.4 Hypothesis

In order to understand the carbon isotope effect preserved in the sedimentary record (ε_{TOC}), this study investigates what factors control the isotope effect associated with the primary production in cyanobacteria (ε_P). Variation in ε_{TOC} values preserved in sedimentary rocks could then provide clues into how cyanobacteria functioned under different atmospheric conditions and when they evolved CCMs.

One critical test of a cyanobacterial ε_P proxy is whether the isotope effect associated with carbon fixation is strain specific. This would make it difficult to interpret the proxy as a general cyanobacterial signal. Here we characterize ε_P values of four cyanobacterial strains that are distributed on the phylogenic tree (i.e., not closely related) to test whether the strain controls ε_P values and if their CCMs function differently.

This study also investigates whether the concentration of CO_2 or the growth rate of the organism affect the isotope fractionation associated with the photosynthetic carbon fixation. Based on the phenomenological model we would expect that ε_p values will be larger in environments with higher CO_2 concentrations and slow growth rates as these conditions would lead to smaller *f* values. Alternatively, fast growth rates and lower CO_2 concentrations would lead to larger *f* values and smaller ε_P values.

These observations will enable me to identify whether the organism (strain), growth rate, or CO_2 concentration controls the net isotope effect associated with carbon fixation in cyanobacteria. Ultimately this experimental work will provide a framework to interpret the geologic carbon isotope record and a way to investigate the evolution of oxygenic photosynthesis and CCMs in cyanobacteria.

Figure 1.5: The phylogenic tree showing the position of cyanobacterial strains that are selected for this experiment: *Gloeomargarita lithophora*, *Synechococcus* sp. PCC 7002, *Synechococcus* sp. PCC 6312, and the possible position of *Neosynechococcus sphagnicola* (Moreira et al., 2017).

2. Background

2.1 The evolution of oxygenic photosynthetic cyanobacteria

The main source of free oxygen released into the atmosphere was produced by cyanobacteria. They appear to be the primary producer that was able to photosynthesize and produce O_2 in the Proterozoic Eon and maybe older than that. The record of carbon isotope fractionation possibly indicates biological carbon fixation more than 3.850 billion years ago (Mojzsis et al., 1996). However, meteorite infalls can also perform this fractionation. Moreover, this record was intensely altered and less evidence of geochemical processes was preserved. Further, it is well supported that the oxygenic photosynthesis evolved well before the Great Oxidation Event (Buick, 2008).

Cyanobacterial mats are commonly found in coastal habitats where they experience low and high tides. They secrete extracellular envelopes to protect the cell inside from high light intensity and dryness during the low tide. Cyanobacterial sheaths are preserved in chert microfossils and are essential tools for paleobiologists to study their morphology. Even though cyanobacteria are not typically preserved in ancient sediments, these carbonate sheaths contain a chemical signal of altered carbon isotope ratios in many sedimentary rocks that represents the biotic processes.

Stromatolites are sedimentary structures built by microbial activities. Stromatolites are uncommon in the present day but can still be found in hypersaline sub-tidal environments. Benthic microbial mats spread across sediment surfaces and grow upward in the photic zone toward the sunlight. Sediments precipitate from the water and are trapped by mucus on top of the upper layer produced by cyanobacteria, which later on will accumulate as a new layer. The bottom of the mats contains dead cells and carbonate that crystallizes. As the process continues, the layers are accreted and form laminated and domed-like structures, which are preserved in sedimentary rocks. However, the texture of Archaean stromatolite (3.5-3.4 billion years old) cannot be distinguished from abiotic processes. They could accrete in anoxic waters and be produced by anoxygenic autotrophs in which sulfide is their electron donor (Knoll Andrew H. et al., 2016). However, carbon isotope fractionation from Proterozoic stromatolites and extracellular sheaths may indicate the biotic product of oxygenic photosynthetic cyanobacteria.

2.3 The carbon isotope system

The record of carbon isotope composition from biosynthetic products could reveal the co-evolution of cyanobacteria and the atmosphere. Carbon isotopes can indicate the difference between biotic and abiotic processes. Carbon has three natural occurring isotopes in which ^{12}C and ^{13}C are stable isotope. About 98.9% of all carbon is in ^{12}C form, while ^{14}C is a radioactive element that decays to ^{14}N. ^{12}C contains six protons and six neutrons for a total molecular weight of twelve while ^{13}C has one extra neutron resulting in a total molecular weight of thirteen. These isotopes require different amounts of kinetic energy for activities because of their differing molecular weights. For that reason, the carbon fixation in biological forms prefers the light isotope of carbon,^{12}C, which results in the strongly depleted ^{13}C organic matter. The physical or chemical process, which acts to separate isotopes, is known as fractionation.

The delta notation of carbon isotopes is expressed in the relationship as follows:

$$\delta^{13}C = \left[\frac{(^{13}C/^{12}C)_{sample} - (^{13}C/^{12}C)_{standard}}{(^{13}C/^{12}C)_{standard}}\right] \times 1000$$

The carbon isotopic difference between biomass preserved in sedimentary rock (TOC) and the carbonate minerals is expressed in term of (ε_{TOC}), which is controlled by several factors including fractionations associated with carbonate minerals, dissolved carbon dioxide, and primary biomass.

Dissolved carbon in the surface ocean join with an oxygen to form a carbonate ion, and combines with metal cations to form carbonate minerals that are usually preserved in the form of sedimentary rock. One carbonate mineral is limestone, which has the largest storage of carbon on the earth's surface. The isotopic depletion of dissolved CO_2 on the surface of the waters relative to sedimentary carbonates is Δ_{carb}.

$$\Delta_{carb} = \delta^{13}C_{CaCO_3} - \delta^{13}C_{CO_2}$$

Meanwhile, the isotopic depletion has two related components, which are the isotopic relationship between dissolved inorganic carbon (DIC) and carbonated minerals differing by 1.2‰, and the temperature-dependent fractionation between dissolved inorganic carbon and dissolved CO_2. The sedimentary record also preserves biomass produced by organisms, but respiratory remineralization could have further isotopic effects. The isotope shift associated with secondary biological processes (Δ_2) is defined as follows:

$$\Delta_2 = \delta^{13}C_{TOC} - \delta^{13}C_{Biomass}$$

Oxygenic photosynthesis by cyanobacteria produces biosynthetic products, which record a characteristic carbon isotope composition. Therefore, the geologic record of carbon isotope fractionation over the geologic timescale could reveal the information about the preferred conditions for cyanobacterial O_2 production.

2.3 The variation of biotic carbon isotope fractionation

Carbon isotope fractionation could also be influenced by the environment and the availability of dissolved carbon dioxide. Carbon isotope fractionation in a hypersaline heliothermal pond has been studied by sampling the isolated cyanobacteria and diatoms at different depths with the known temperature and salinity condition. This hypersaline habitat has experienced the extremely reduced solubility of carbon dioxide due to high salinity increasing with depth. Therefore, there is no production of O_2 at the lower depth due to low CO_2 availability and low light transmission. The carbon isotope composition of organic matter in the uppermost layer is relatively light because dissolved CO_2 coming from the atmosphere allows cyanobacteria to be selective for lighter carbon isotopes. The carbon isotope composition of organic matter in the middle layer is heaviest because there is high competition for CO_2 in the limited CO_2 environment. Therefore, the mechanism cannot be selective over lighter carbon preferences, which results in the heavy isotope relatively resembling atmospheric carbon isotopes. Meanwhile, the carbon isotopes at the bottommost layer have relatively light isotopes and there is no indication of O_2 production. Likely the uppermost cyanobacteria died and sank to the bottom. Therefore, the availability of dissolved carbon dioxide affects the carbon isotope variation in the organic matter.

2.4 The position of selected cyanobacterial strains on the phylogenic tree

Genomes, physical fossils, biomarkers, and isotope geochemistry also suggest that oxygenic photosynthesis evolved within the cyanobacteria stem lineage (Betts et al., 2018). As mentioned earlier, cyanobacteria possess carboxysomes, which is a part of their concentrating mechanism. There are two types of carboxysomes: alpha and beta. The α carboxysome encapsulates a form 1A RubisCO, and the β carboxysome

encapsulates a from 1B RubisCO. All cyanobacterial strains studied here possess β carboxysome and 1B RubisCO. According to the phylogenic tree, it seems like β carboxysomes are the more ancestral form.

Based on phylogenomic evidence of the early origin of plastids, the closest relative of ancestral cyanobacteria is *Gloeomargarita* lithophora (Ponce-Toledo et al., 2017; Sánchez-Baracaldo et al., 2017a). *Gloeomargarita* lithophora was initially found in an alkali crater lake in Mexico. The chemistry of Alchichica crater Lake is magnesium-rich water and oversaturated with calcium and magnesium carbonated with pH about 8.9 (Benzerara et al., 2014). Moreover, *Gloeomargarita* lithophora is able to form intracellular Ca carbonates (Couradeau et al., 2012).

3. Materials and Methods

3.1 Culturing

3.1.1 Strains

Four cyanobacterial strains, *Gloeomargarita lithophora (G. lithophora)*, *Synechococcus* sp. PCC 7002 (*Synechococcus* 7002), *Synechococcus* sp. PCC 6312 (Synechococcus 6312), and *Neosynechococcus sphagnicola (N. sphagnicola)* were used for this experiment. Liquid pre-cultures of *Gloeomargarita lithophora*, *Synechococcus* sp. PCC 6312 and *Neosynechococcus sphagnicola* were grown in BG11 medium (see appendix A) in air at 30˚C. *Synechococcus* sp. PCC 7002 was inoculated from an A+ medium agar plate.

3.1.2 Media Preparation

All experiments were performed in a freshwater BG11 medium, containing 17.60 mM of Sodium nitrate ($NaNO_3$), 0.175 mM of Potassium phosphate dibasic trihydrate ($K_2HPO_4\ 3H_2O$), 0.3 mM of Magnesium sulfate heptahydrate ($MgSO_4\ 7H_2O$), 0.24 mM of Calcium chloride dihydrate ($CaCl_2\ 2H_2O$), 0.31 mM of Citric Acid Anhydrous, 0.023 mM of Ferric Ammonium Citrate, 0.0028 mM of Ethylenedinitrilotetraacetic acid (EDTA) disodium salt dehydrate ($Na_2EDTA\ 2H_2O$), 10 ml/L of HEPEs buffer, and 1 ml/L of trace minerals (see appendix A). We compared the recipes for three different preparations of BG11, one commercial and two laboratory versions before deciding on a preparation protocol (see appendix B). Typically, BG11 medium contains 0.19 mM of Na_2CO_3; however, we removed the Na_2CO_3 in our preparation to avoid the confounding presence of multiple carbon sources with different carbon isotope compositions. All BG11 medium was autoclaved, allowed to cool to room temperature, and stored in the dark. We prepared the growth medium in large batches to avoid variation in the media composition within each experiment. The growth medium was supplemented with vitamin B12 with a concentration of 1 µl/ml before inoculating.

3.1.3 Experimental setup

All culturing was performed in the Cameron Laboratory at CU Boulder. Cyanobacterial cultures were grown in autoclaved 125 ml Erlenmeyer flasks containing 30 ml of BG11 medium with a foam stopper. Three biological replicates of each strain were inoculated with 2.5-4.0×10^7 cells (1-3% of the final cell count).

All cultures were grown in a Percival incubator model AL-41L4 (Percival Scientific, Iowa, USA), shaking at 130 rpm. In this incubator, the minimum light setting resulted in light levels levels of 33 µmol photons m^{-2} s^{-1}. However, previous culturing experience suggests that the optimal light level for *G. lithophora* is ~10 µmol photons m^{-2} s^{-1}. We therefore added a 3–mm thick opaque plexiclass filter to lower light intensity. We measured the light level at each position in the shaker (VWR Scientific, Pennsylvania, USA) to determine the variability in light levels between biological replicates (Table 3.1). Strains and replicates remained in the same position in the shaker across all experiments. Light levels varied by up to 12%.

Table 3.1: Light levels at each position in the shaker in µmol photons m^{-2} s^{-1}.

N.sphagnicola Rep1 8.64 μmol	*N.sphagnicola* Rep2 9.70 μmol	*N.sphagnicola* Rep 3 10.03 μmol
G. lithophora Rep 1 9.84 μmol	*G. lithophora* Rep 2 10.72 μmol	*G. lithophora* Rep 3 10.69 μmol
PCC 7002 Rep 1 8.38 μmol	PCC 7002 Rep 2 9.45 μmol	PCC 7002 Rep 3 9.82 μmol
PCC 6312 Rep 1 8.48 μmol	PCC 6312 Rep 2 9.20 μmol	PCC 6312 Rep 3 9.40 μmol

Cyanobacterial growth was monitored by measuring the optical density (OD) of a 200 µl culture suspension at 730 nm. The $OD_{730\ nm}$ was measured periodically using a photometer or a plate reader (TECAN, Männedorf, Switzerland). The culture $OD_{730\ nm}$ was determined by subtracting the $OD_{730\ nm}$ of a medium blank from the initial $OD_{730\ nm}$ reading. I converted $OD_{730\ nm}$ measurements to cell density (ρ) in cells ml^{-1} using an

existing calibration based on *Synechococcus* 7002. The relationship between cell density (ρ) and optical density at 730 nm ($OD_{730\ nm}$) for *Synechococcus* 7002 is described in Equation 3.1.

(3.1) $$\rho = [(7.4\times10^{8})\times OD_{730}] - 1.2\times10^{7}$$

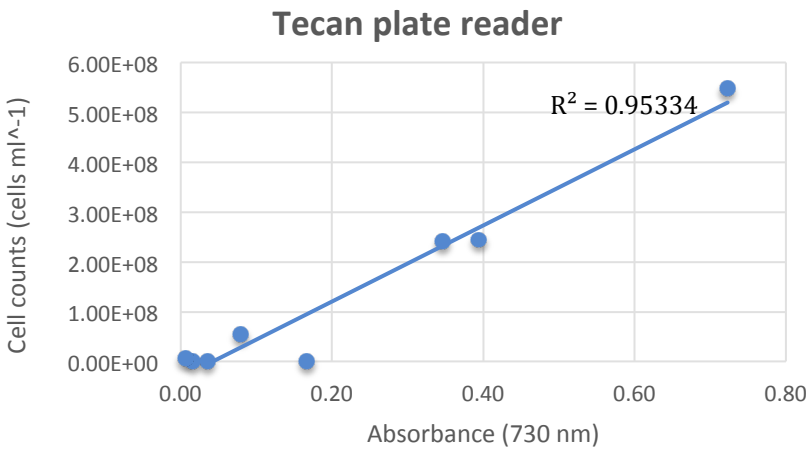

Figure 3.1: The plate reader calibration from *Synechococcus* sp. PCC 7002 at temperature of 37˚C

Cultures were harvested at an $OD_{730\ nm}$ of 0.18-0.22, corresponding to a cell density of $2.5\text{-}4.0\times10^{7}$ cells ml $^{-1}$. A typical bacterial growth curve can be divided into phases. In lag phase the culture is adjusting to the new environmental conditions and the increase in cell density is not measurable by $OD_{730\ nm}$. In log phase the cell density increases exponentially with time. We harvested cultures before they reached linear or stationary phase in an effort to normalize growth rates and growth phase between different strains and experimental conditions (Figure 3.2). We calculated a net growth rate (μ) using the total change in cell density (ρ) per unit time (t).

(3.2) $$\mu = \frac{\rho_{final} - \rho_{initial}}{t}$$

3.1.4 Varying CO_2 levels

The goal of this project was to observe how carbon isotope fractionation by cyanobacteria responds to varying CO_2 concentrations. All strains were grown as

described above in air and 3% CO_2, except *G. lithophora*, which did not grow in 3% CO_2. We calculated the concentration of dissolved CO_2 in the culture medium. The amount of dissolved carbon dioxide depends on temperature, salinity, total pressure, partial pressure of gaseous carbon dioxide, and pH. The total pressure was 0.821 atm. The partial pressure of carbon dioxide was 0.0003284 atm in air and 0.02463 atm in 3% CO_2. This corresponded to a dissolved CO_2 concentration of 9.81 μmol/kg in air and 735.55 μmol/kg in 3% CO_2.

We acclimated cyanobacterial cultures in each CO_2 setting using 3-4 serial transfers. The serial cultures allowed us to observe how cyanobacteria acclimated to each environment and to reduce the amount of biomass from the pre-cultured cells, which the initial inoculum left 6-10% in Acclimation 3, and 2-3 % left in Acclimation 4.

Cultures suspensions were stored in the ultra-low temperature freezer (VWR Scientific, Pennsylvania, USA) at -70˚C prior to analysis. Cultures were harvested by centrifugation and washed with ultrapure water. Sample aliquots were pipetted into pre-weighed tin capsules and dried for 12 hours at 50°C.

3.2 Measuring the carbon isotope composition

3.2.*1 Measuring the carbon isotope composition of cyanobacterial biomass*

Variations in the isotope ratios of naturally occurring materials are reported as δ-values. The carbon isotope composition of cyanobacterial biomass was measured in the Earth Systems Stable Isotope Lab at the University of Colorado Boulder. Samples were oxidized and combusted with a Thermo Scientific Flash Elemental Analyzer and the resultant CO_2 was then analyzed with a Thermo Scientific Delta V Isotope Ratio Mass Spectrometer.

The δ-values are commonly expressed in parts per thousand (per mil or ‰) difference from the internationally agreed zero points or VPDB standard (Vienna Peedee Belemnite) for $^{13}C/^{12}C$.

(2.1) $$\delta^{13}C_{sample} = \left[\frac{(^{13}C/^{12}C)_{sample} - (^{13}C/^{12}C)_{standard}}{(^{13}C/^{12}C)_{standard}}\right] \times 1000$$

To attain precision and accuracy in using continuous flow IRMS, several standards were used for correction in the elemental analysis. The linearity standard were run in the beginning of the analytical run and was used to correct for changes in

instrument sensitivity that may occur because of variable sample size and pressure. Drift standards and the monitoring standards were run for every six samples. The drift standards were used to monitor the change in the instrument sensitivity over the course of an analytical run. The monitoring standards were treated as samples and should match the known value after correction. Acetanilide (University of Indiana; $\delta^{13}C$ of -29.53$\pm$0.01‰; weight %C of 71.09) was used to correct for linearity and drift. Ethylene diamine tetraacetic acid (EDTA2; $\delta^{13}C$ of -40.38 $\pm$ 0.01‰; weight %C of 41.09) was used as a monitoring standard and pugel ($\delta^{13}C$ of -12.62‰; weight% C 44.02) as a discrimination standard.

3.2.*2 Measuring the carbon isotope composition of CO_2 gas*

Isotopic analysis of CO_2 gas was conducted in the Earth Systems Stable Isotope Lab at the University of Colorado Boulder. The CO_2 was analyzed with a Thermo Scientific Delta V Isotope Ratio Mass Spectrometer. Ratios are expressed as $^{13}C/^{12}C$ in units of relative per mil (‰) difference between the sample (R_{sample}) and a standard ($R_{standard}$,) of Vienna Peedee Belemnite (VPBD) (Equation 2.1). A correcting standard of HIS ($\delta^{13}C$ of -4.8 ‰ in VPBD) was used to correct for linearity and drift.

3.3 Determining the concentration and carbon isotope composition of inorganic C

3.3.1 The concentration of dissolved carbon dioxide

Dissolved inorganic carbon (DIC) exists in three forms: as aqueous carbon dioxide (CO_{2aq}), bicarbonate (HCO_3^-), and as carbonate ions (CO_3^{2-}). In the experiments performed here, we knew the volume:volume ratio of CO_2 in the incubator and calculated the concentration of DIC species using the pH, temperature, pressure, and salinity of the culture medium.

The concentration of DIC species was calculated from a csys.m function developed by Richard E. Zeebe and Dieter A. Wolf-Gladrow to calculate the concentration of DIC species in seawater (Zeebe and Wolf-Gladrow, 2001). The function required as inputs the temperature, salinity, and total pressure of the system. We also provided pH and the partial pressure of carbon dioxide as the two known variables in the DIC system. We knew the experimental temperature from the incubator (30˚C). Salinity

was calculated to be 0 from the concentration of Na^+ and Cl^- in the media (CO2calculator_ver7.xls). The total pressure in Boulder was obtained from the University of Colorado ATOC Weather Network (http://foehn.colorado.edu/weather/atoc1/). We measured the pH of cultures (7.47 in air and 6.91 in 3% CO_2) by removing the cultures from the incubator and immediately measure pH. The partial pressure of CO_2 was determined by the volume: volume ratio of CO_2:air in the incubator. The csys.m function returns the concentration of $CO_2, HCO_3^-, CO_3^{2-}, DIC, Alk$, the partial pressure of CO_2, the fugacity of CO_2, the total pH, and the pH of free hydrogen ions. The full calculations of csys.m are listed in appendix C.

3.4 Calculating the isotopic fractionation associated with primary production (ε_P)

The isotope fractionation associated with primary production (ε_P) can be define as the isotopic difference between dissolved CO_2 and primary biomass:

(3.3) $$\varepsilon_P \equiv \delta^{13}C_{CO_{2(aq)}} - \delta^{13}C_{biomass}$$

Aqueous carbon dioxide in the media, which is dissolved carbon dioxide that constantly exchanges with atmosphere. The value of the carbon isotope fractionation between aqueous carbon dioxide and atmospheric carbon dioxide is temperature dependence, which the relationship is given as follows:

(3.4) $$\varepsilon_{CO_{2(aq)}-CO_{2(g)}} = 0.0049T_c - 1.31‰$$

In which T_c is the temperature in ˚C. In other way, the fractionation factor can be arranged in the form of the value of the carbon isotope fractionation, results in:

(3.4) $$\propto_{CO_{2(aq)}-CO_{2(g)}} = \frac{\varepsilon_{CO_{2(aq)}-CO_{2(g)}}}{1000} + 1$$

The fractionation factor ($\propto$) between aqueous carbon dioxide and atmospheric carbon dioxide can be written as follows:

(3.5) $$\propto_{CO_{2(aq)}-CO_{2(g)}} = \frac{\delta^{13}C_{CO_{2(aq)}}+1000}{\delta^{13}C_{CO_{2(g)}}+1000}$$

According to the two relationships above, the isotopic composition of aqueous carbon dioxide can be determined by rearranging the equation to:

(3.6) $$\delta^{13}C_{CO_{2(aq)}} = \left[\propto_{CO_{2(aq)}-CO_{2(g)}} \times \left(\delta^{13}C_{CO_{2(g)}} + 1000\right)\right] - 1000$$

The primary production by cyanobacteria takes aqueous carbon dioxide into the cell and synthesizes organic carbon to produce biomass. In order to determine the isotope fractionation by the primary production, the isotopic composition of aqueous carbon dioxide of is obtained from the equation above, and the isotopic composition of biomass is obtained from the mass spectrometry after correcting with standards (*d13C.disc)*.

(3.7) $$\varepsilon_{CO_{2(aq)}-biomass} = \varepsilon_p = \left(\frac{\delta^{13}C_{CO_{2(aq)}}+1000}{\delta^{13}C_{biomass}+1000} - 1\right) \times 1000$$

4. Results

4.3 Cyanobacterial culturing

Four cyanobacterial strains, *Gloeomargarita lithophora*, *Synechococcus* sp. PCC 7002, *Synechococcus* sp. PCC 6312, and *Neosynechococcus sphagnicola* had been culturing in a freshwater BG11 medium under low light intensity and at temperature of 30˚C. Cyanobacteria were grown under air and 3% CO_2. We acclimated cyanobacterial cultures in each CO_2 setting using 3-4 serial transfers to observe how cyanobacteria acclimated to each environment and to reduce the amount of biomass from the pre-cultured cells.

However, *G. lithophora* did not grow under high CO_2. One possible explanation is that *G. lithophora* could not grow in the high CO_2 conditions due to the pH. The pH of growth medium at 3% CO_2 was 6.91, while G. lithophora was isolated from an alkaline lake with a pH of 8.9.

The error bars plotted on the figures represent the standard deviation from each cyanobacterial strain in either air or 3% CO_2 condition. We then plotted these error bars on each individual data point. The variation of the net growth rate is similar for every cyanobacterial strain. The possible causes could come from the light variation in the incubator. Cyanobacteria that received slightly higher light intensity grew faster. The uncertainties in the isotope effect for all cyanobacteria are fairly consistent, except for *Gloeomargarita lithophora*. *Gloeomargarita lithophora* has the highest uncertainty (26.30 ±2.29 ‰). During the acclimations, most of *Gloeomargarita lithophora* cultures were harvested early, because the cultures reached the stationary phase before the optical density at 730-nm wavelength reached 0.2. Therefore, the variation in the isotope effect possibly results from cyanobacteria reaching in stationary phase. However, it is hard to determine uncertainty for the concentration of dissolved carbon dioxide, as it was calculated from the provided carbon dioxide percentage in the environment. Therefore, under the same condition, the concentration of carbon dioxide dissolved in the media was equal for all strains.

The net growth rate (Equation 3.2) of individual strains was generally consistent across acclimations (Figure 4.1). This consistency suggests that the cyanobacterial strains quickly acclimated to each environmental setting. We therefore determined ε_p values for all acclimations and have included all acclimations in the data analysis.

Net growth rates did not appear to depend strongly on CO_2 conditions (Appendix D). If the cultures were carbon limited, the growth rate of each strain should increase as a function of CO_2 concentration, as CO_2 is fixed to produce cellular biomass. In fact, the net growth rates of *Synechococcus* 7002 and *N. sphagnicola* did not change when the concentration of dissolved carbon dioxide increased (Figure 4.1). However, the net growth rate of *Synechococcus* 6312 was slightly faster at under 3% CO_2 (Figure 4.1).

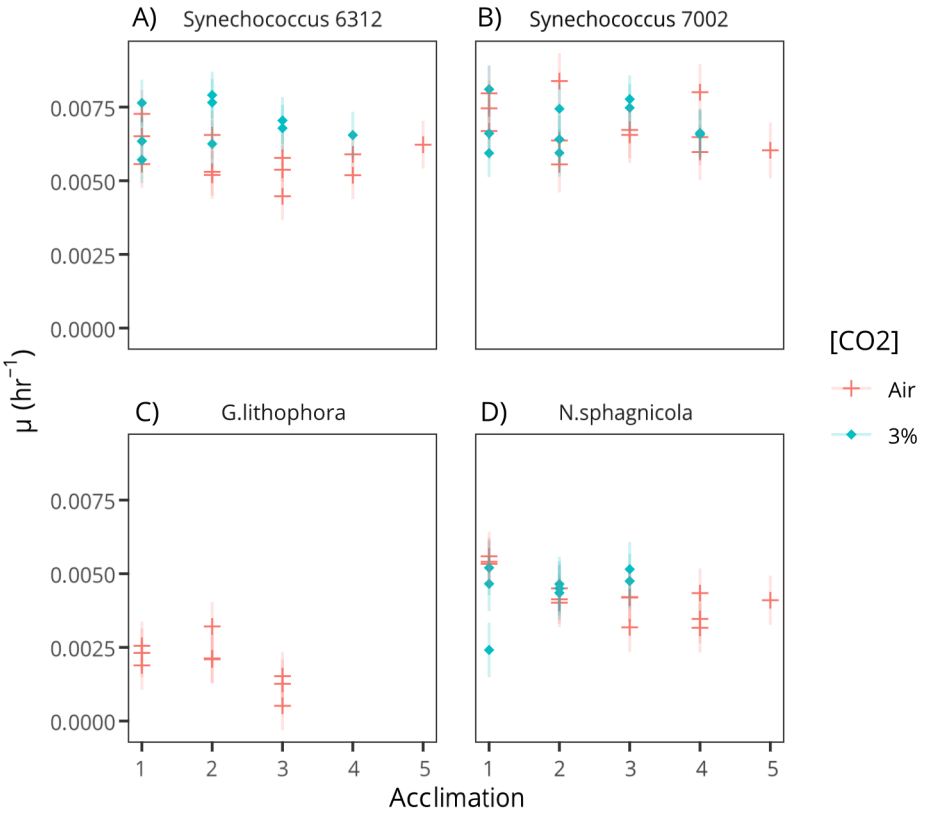

Figure 4.1: The net growth rates of cyanobacterial strains A) *Synechococcus* sp. PCC 6312, B) *Synechococcus* sp. PCC 7002, C) *Gloeomargarita lithophora* and D) *Neosynechococcus sphagnicola*, while acclimating under air condition (red crosses) and under 3% CO_2 condition (blue circles). Error bars represent the standard deviation of growth rates from biological replicates under different CO_2 conditions.

4.4 Isotopic results

We determined the net isotope effect associated with primary productivity (ε_P) for all strains across all acclimations. Values of ε_p were calculated according to Equation 3.7 after $\delta^{13}C_{CO_{2(g)}}$ and $\delta^{13}C_{biomass}$ values were measured in the CU Boulder Earth Systems Stable Isotope Lab. Based on the phenomenological model, we would expect ε_p to have a relationship with the net growth rate of each culture and the availability of carbon dioxide in the environment. Based on the *f* value, the proportion of carbon fixed versus removed from the reaction site, we would expect less fractionation at fast growth rates and low CO_2 concentrations.

Consistent with this prediction, ε_p values decrease with increasing growth rates across all cyanobacterial strains grown in air (Figure 4.2). While the net growth rate varies between strains, there appears to be a single relationship between ε_p values and the net growth rate of cyanobacteria. As outlined in the introduction that the four strains are not closely related (Figure 1.5), this single relationship between εp and growth rate potentially suggests a uniform underlying physiology.

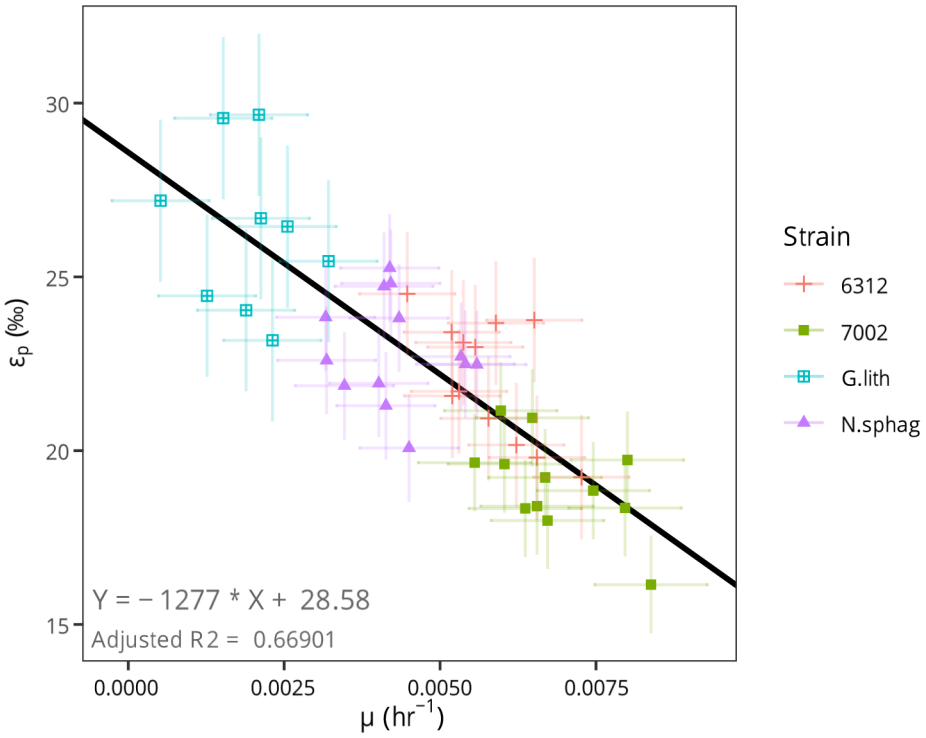

Figure 4.2: The isotope effect associated with primary production (ε_P) as a function of the net growth rate of cyanobacterial strains growing in air. Horizontal and vertical error bars represent standard deviation of growth rate and ε_p from biological replicates in air.

In contrast, ε_P values do not decrease with increasing CO_2 concentrations (Figure 4.3). Values of ε_P are generally consistent between cultures grown in air and 3% CO_2. These cultures are energy, or light limited, rather than carbon limited as light intensity variation resulted in some replicates growing faster than others. Since these cultures do not appear to be carbon limited, and CO_2 appears to be in excess, we would not expect increasing the CO_2 levels further would prompt a physiological response. As ε_P values show no correlation with increasing CO_2 concentrations, our results support the idea that the amount of dissolved carbon dioxide in the system does not affect the isotope fractionation associated with primary production of cyanobacteria.

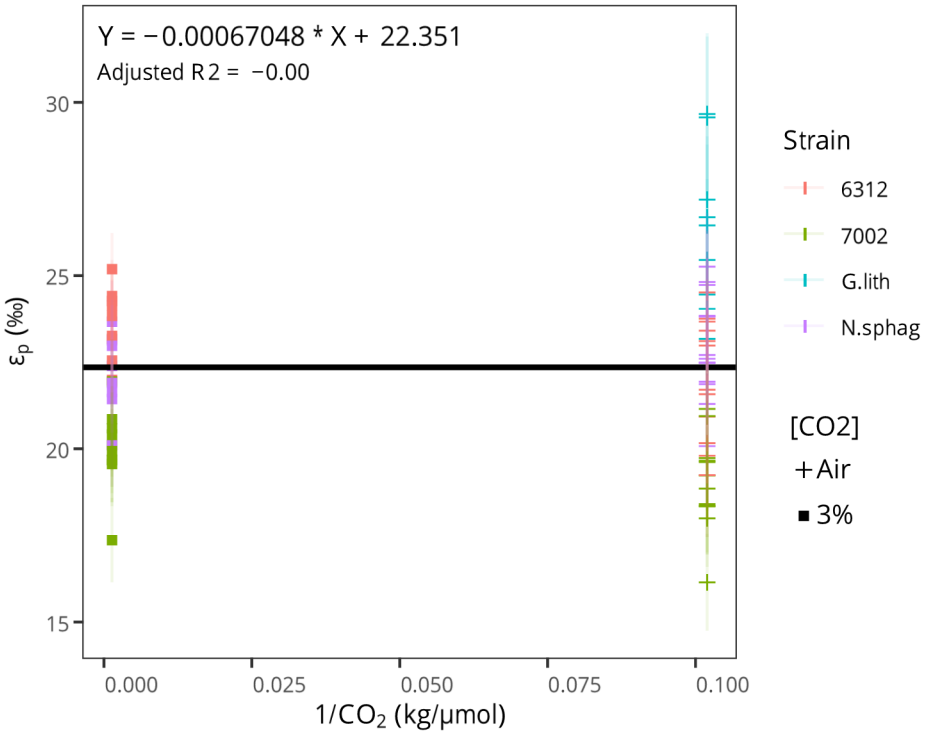

Figure 4.3: The isotope effect associated with primary production (ε_P) as a function of the inverse of carbon dioxide concentration. Error bars represent standard deviation ε_P from biological replicates under different CO_2 conditions.

When considered together, the relationship between ε_P and net growth rate appears to be dominant over the relationship between ε_P and CO_2 levels in light limited cultures (Figure 4.4). For *N. sphagnicola,* and *Synechococcus* 7002 values of ε_P in 3% CO_2 conditions are consistent with the relationship between ε_P and net growth rate observed in air (Figure 4.4). This is consistent with the idea of an energy limited system in which increasing CO_2 concentrations do not affect net growth rate or the proportion of carbon being fixed (*f* value). However, ε_P values for *Synechococcus* 6312 growing in 3% CO_2 are not entirely consistent with the observed relationship between ε_P and net growth rate (Figure 4.4). Here ε_P values and growth rates are larger than those values observed in air.

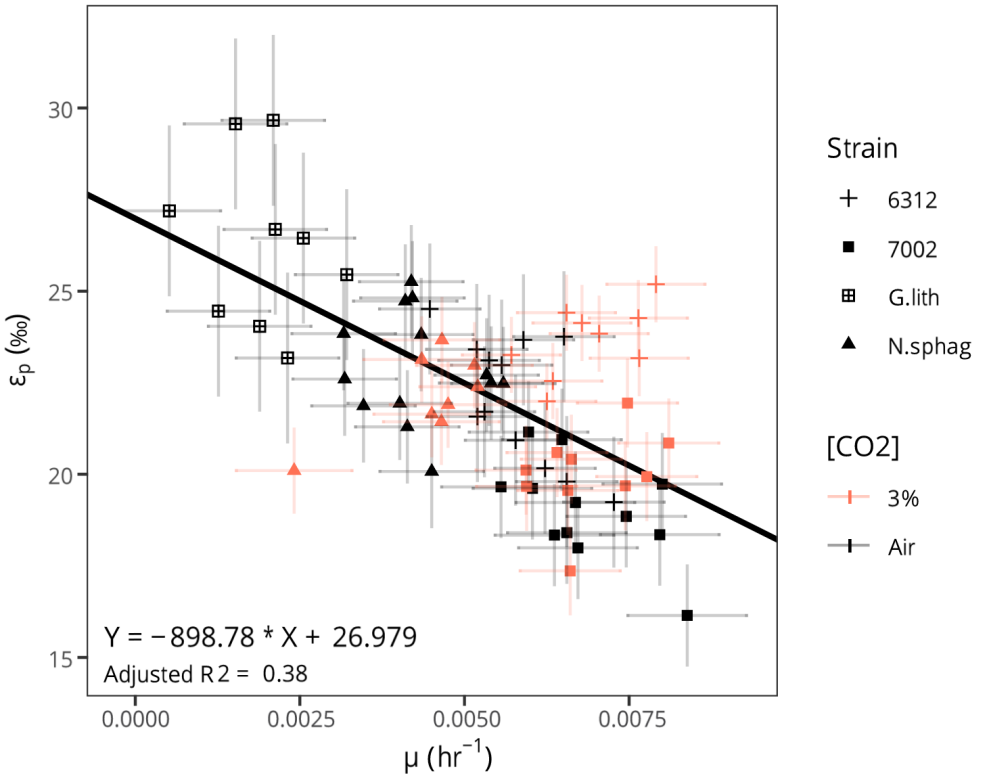

Figure 4.4: The isotope effect associated with primary production (ε_P) as a function of the net growth rate of cyanobacterial strains growing in air and 3% CO_2. Horizontal and vertical error bars represent standard deviation of growth rate and ε_P from biological replicates under each CO_2 concentration.

The net growth rates of *Synechococcus* sp. PCC 6312 increases when a dissolved carbon dioxide levels increase (Figure 4.5). This relationship is consistent with our prediction that high CO_2 level will increase the growth rate of cyanobacteria. Therefore, carbon dioxide may be limiting in this experiment for *Synechococcus* sp. PCC 6312. It is interesting that the isotope effect associated with primary production increases when the net growth rate increases. One possible explanation is that the isotope effect associated with primary production of *Synechococcus* sp. PCC 6312 is dominated by the availability of carbon in the environment. Under 3% CO_2 condition, cyanobacteria can take a small fraction of available carbon, which results in a larger fractionation.

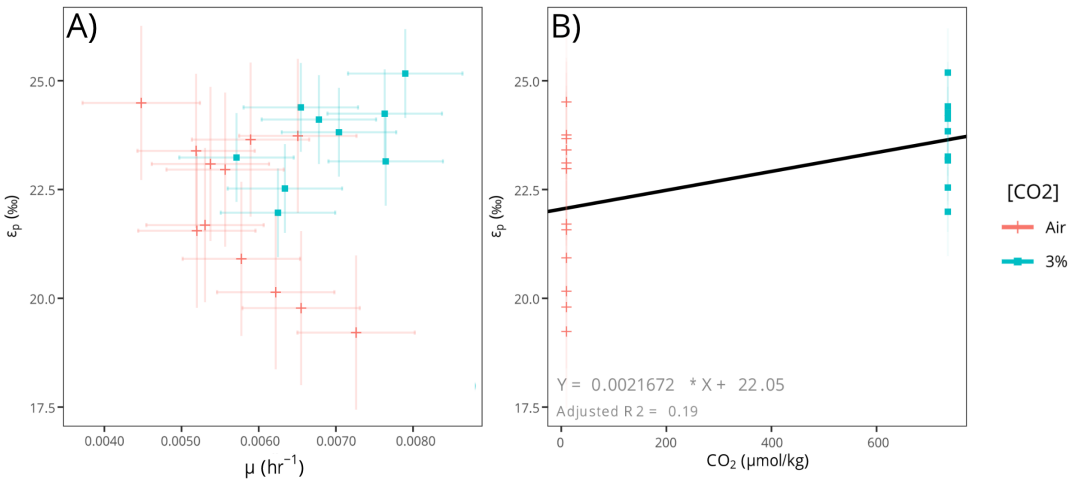

Figure 4.5: A) the isotope effect associated with primary production (ε_P) as a function of the net growth rate of *Synechococcus* sp. PCC 6312 growing under air and 3% CO2 conditions, B) the isotope effect associated with primary production (ε_P) *Synechococcus* sp. PCC 6312 as a function of dissolved carbon dioxide levels. Horizontal and vertical error bars represent standard deviation of growth rate and ε_P from biological replicates under each CO_2 concentration.

Table 4.1: The mean isotope effect associated with the primary production and the net grown rate of four cyanobacteria strains under air and 3% CO_2 conditions. The uncertainty represents the standard deviation of growth rate and ε_P from biological replicates under each CO_2 concentration.

Condition	**Cyanobacterial Strain**	**ε_P (‰)**	**μ (hr^{-1})**
Air	*Synechococcus sp. PCC 7002*	19.03 ±1.35	0.00685 ±0.00076
Air	*Synechococcus sp. PCC 6312*	22.07 ±1.74	0.00578 ±0.00090
Air	*N. sphagnicola*	22.91 ±1.50	0.00428 ±0.00079
Air	*Gloeomargarita lithophora*	26.30 ±2.29	0.00194 ±0.00078
3% CO_2	*Synechococcus sp. PCC 7002*	20.01 ±1.17	0.00689 ±0.00076
3% CO_2	*Synechococcus sp. PCC 6312*	23.64 ±1.00	0.00688 ±0.00074
3% CO_2	*N. sphagnicola*	22.15 ±1.14	0.00446 ±0.00088

5. Discussion

5.1 The dependence of ε_p values on net growth rate

The four cyanobacterial strains investigated here showed a single linear response in ε_P values to increasing net growth rates. This relationship suggests that underlying physiology may control ε_P values. Moreover, ε_P values do not appear to be strain-specific. One common physiological feature of all strains studied here is the presence of a carbon concentrating mechanism, or CCM. However, these results are specific to cyanobacteria growing in a light-limited environment.

While the response of ε_p values to growth rates seems to form one consistent relationship across all strains, there were differences between how the strains responded to changes in CO_2 conditions. For *N. sphagnicola,* and *Synechococcus* 7002, growth rates did not increase at higher CO_2 concentrations. This is consistent with light-limiting rather than carbon-limiting conditions. We would predict that increasing light-levels would lead to increased growth rates and smaller ε_P values. Individual cultures responded to small differences in light levels (up to 12% light variation) between biological replicates. During the acclimations, cultures growing on the right side of the incubator received a little higher light intensity tended to grow faster. Therfore we suspect that the growth rate depends on light intensity, and light is limiting in this experiment.

As reported earlier, we do not have ε_P values for *G. lithophora* in 3% CO_2 as it would not grow in these conditions. We hypothesize that *G. lithophora* experienced pH shock because it was isolated from an alkaline lake with pH of 8.9 (Kaźmierczak et al., 2011), while the pH of the growth medium was 6.91 when the incubator transitioned to 3% CO_2. While we cannot conclude the relationship between ε_P, growth rate and CO_2 concentration in *G. lithophora*, it seems plausible that it would follow the ε_P vs. growth rate response observed in the other strains.

In contrast to the other strains, the growth rate of *Synechococcus* 6312 increased at the higher concentration of CO_2. This suggests that *Synechococcus* 6312 may have been more carbon-limited than the other strains in our experimental conditions. Given the correlation between ε_P values and net growth rate, we would expect faster growth rates to result in smaller ε_P values in this high CO_2 condition. However, ε_P values for

Synechococcus 6312 did not decrease, potentially suggesting that CO_2 concentration, rather than growth rate, were the dominant control on ε_P values in this condition.

5.2 Implications for the use of carbon isotopes as a proxy for cyanobacteria

In this study, we investigated whether the isotope effect associated with primary production by cyanobacteria (ε_P) is controlled by the cyanobacterial strain, the concentration of CO_2, or the growth rate. We found that net growth rate was the controlling factor for ε_p values across four cyanobacterial strains under light-limiting conditions. However, this may not be the case for different conditions, for example cultures experiencing carbon limitation. Based on the phenomenological model, we might expect different results, *i.e.*, a stronger dependence of ε_P on CO_2 availability, if these experiments were performed in carbon limited conditions.

Ultimately, we aim to understand the factors controlling carbon isotope fractionation by cyanobacteria across a range of environmental conditions. This will inform the interpretation of ε_P and ε_{TOC} values in the geologic record. Here, we have explored light-limiting conditions at both modern and 100 times present atmospheric levels of pCO_2 (Kaufman and Xiao, 2003). In order to better understand the possible range of ε_P values produced by cyanobacteria we could grow them at saturating light-levels and then varying CO_2. Understanding the factors controlling ε_P values in cyanobacteria in different environmental conditions will provide a framework to use the carbon isotope record to investigate the evolution of cyanobacteria, particularly in the context of the GOE.

5.3 Remaining questions

The relatinoship between ε_P and growth rate observed here agrees with the phenomenological model based on C3 plants. This is somewhat surprising given the presence of a CCM in all cyanobacterial strains studied here and the absence of a CCM in the phenomenological model. Yet the timing of the evolution of CCMs in cyanobacteria remains unknown with estimates spaning 400 Ma to 2.4 Ga (Badger et al., 2002; Raven John A. et al., 2012; Raven et al., 2017). In order to apply the results of our work to the geologic carbon isotope record, we need to know when CCMs evolved or additionally

characterize carbon isotope fractionation by cyanobacteria without CCMs. Moreover, in the experiments performed here, the four cyanobacterial strains possess β −carboxysomes. It would helpful to understand whether cyanobacteria that possess α − and β −carboxysome fractionate carbon isotope differently.

Finally, it's been suggested that cyanobacteria inhabited freshwater habitats prior to the plastid endosymbiotic event (Sánchez-Baracaldo et al., 2017b). Given this hypothesis, it would be interesting to determine whether freshwater and marine environment affect carbon isotope fractionation by cyanobacteria.

6. Conclusions

We have determined the controlling factor on ε_P values in light-limited conditions under Proterozoic CO_2 conditions. The major finding of this study is that ε_p values across four cyanobacterial strains were dominantly controlled by growth rate, rather than cyanobacterial strain or the concentration of CO_2. These findings will allow us to interpret the geologic carbon isotope record and ε_{TOC} values throughout the Proterozoic, before the rise of Eukaryotes, when cyanobacteria were thought to be the dominant primary producers. We could use this ε_p proxy specific to cyanobacteria to investigate evolution of oxygenic photosynthesis. In future work, we need to understand the controlling factor(s) on ε_p in other environmental conditions as Earth's surface environment has changed over the past 4.6 Ga.

References

Altermann W. and Kazmierczak J. (2003) Archean microfossils: a reappraisal of early life on Earth. *Research in Microbiology* **154**, 611–617.

Badger M. R., Hanson D. and Price G. D. (2002) Evolution and diversity of CO2 concentrating mechanisms in cyanobacteria. *Functional Plant Biol.* **29**, 161–173.

Bekker A., Holland H. D., Wang P.-L., Rumble D., Stein H. J., Hannah J. L., Coetzee L. L. and Beukes N. J. (2004) Dating the rise of atmospheric oxygen. *Nature* **427**, 117–120.

Benzerara K., Couradeau E., Gérard E., Tavera R., Lopez-Archilla A. I., Moreira D. and Lopez-Garcia P. (2014) Geomicrobiological study of modern microbialites from Mexico: towards a better understanding of the ancient fossil record. *BIO Web of Conferences* **2**. Available at: https://doi.org/10.1051/bioconf/20140202002.

Betts H. C., Puttick M. N., Clark J. W., Williams T. A., Donoghue P. C. J. and Pisani D. (2018) Integrated genomic and fossil evidence illuminates life's early evolution and eukaryote origin. *Nature Ecology & Evolution* **2**, 1556–1562.

Bidigare R. R., Fluegge A., Freeman K. H., Hanson K. L., Hayes J. M., Hollander D., Jasper J. P., King L. L., Laws E. A., Milder J., Millero F. J., Pancost R., Popp B. N., Steinberg P. A. and Wakeham S. G. (1997) Consistent fractionation of 13C in nature and in the laboratory: Growth-rate effects in some haptophyte algae. *Global Biogeochemical Cycles* **11**, 279–292.

Buick R. (2008) When did oxygenic photosynthesis evolve? *Philosophical transactions of the Royal Society of London. Series B, Biological sciences* **363**, 2731–2743.

Butterfield N. J., Knoll A. H. and Swett K. (1990) A Bangiophyte Red Alga from the Proterozoic of Arctic Canada. *Science* **250**, 104–107.

Canfield D. E. (2004) THE EARLY HISTORY OF ATMOSPHERIC OXYGEN: Homage to Robert M. Garrels. *Annu. Rev. Earth Planet. Sci.* **33**, 1–36.

Couradeau E., Benzerara K., Gérard E., Moreira D., Bernard S., Brown G. E. and López-García P. (2012) An Early-Branching Microbialite Cyanobacterium Forms Intracellular Carbonates. *Science* **336**, 459.

Crockford P. W., Kunzmann M., Bekker A., Hayles J., Bao H., Halverson G. P., Peng Y., Bui T. H., Cox G. M., Gibson T. M., Wörndle S., Rainbird R., Lepland A., Swanson-Hysell N. L., Master S., Sreenivas B., Kuznetsov A., Krupenik V. and Wing B. A. (2019) Claypool continued: Extending the isotopic record of sedimentary sulfate. *Chemical Geology* **513**, 200–225.

Dick G. J., Grim S. L. and Klatt J. M. (2018) Controls on O2 Production in Cyanobacterial Mats and Implications for Earth's Oxygenation. *Annu. Rev. Earth Planet. Sci.* **46**, 123–147.

Douzery E. J. P., Snell E. A., Bapteste E., Delsuc F. and Philippe H. (2004) The timing of eukaryotic evolution: Does a relaxed molecular clock reconcile proteins and fossils? *Proceedings of the National Academy of Sciences of the United States of America* **101**, 15386–15391.

Goericke R., Montoya J. P. and Fry B. (1994) Physiology of isotopic fractionation in algae and cyanobacteria. In *Stable isotopes in ecology and environmental science* (eds. K. Lajtha and R. H. Michener). Methods in ecology. Blackwell Scientific Publications, Oxford; Boston. pp. 187–221.

Guy R. D., Fogel M. L. and Berry J. A. (1993) Photosynthetic Fractionation of the Stable Isotopes of Oxygen and Carbon. *Plant Physiology* **101**, 37–47.

Hayes J. M., Strauss H. and Kaufman A. J. (1999) The abundance of 13C in marine organic matter and isotopic fractionation in the global biogeochemical cycle of carbon during the past 800 Ma. *Chemical Geology* **161**, 103–125.

Kaufman A. J. and Xiao S. (2003) High CO2 levels in the Proterozoic atmosphere estimated from analyses of individual microfossils. *Nature* **425**, 279.

Kaźmierczak J., Kempe S., Kremer B., López-García P., Moreira D. and Tavera R. (2011) Hydrochemistry and microbialites of the alkaline crater lake Alchichica, Mexico. *Facies* **57**, 543–570.

Knoll A. H., Bergmann K. D. and Strauss J. V (2016) Life: the first two billion years. *Philosophical Transactions of the Royal Society B: Biological Sciences* **371**.

Knoll Andrew H., Bergmann Kristin D. and Strauss Justin V. (2016) Life: the first two billion years. *Philosophical Transactions of the Royal Society B: Biological Sciences* **371**, 20150493.

Krissansen-Totton J., Buick R. and Catling D. C. (2015) A statistical analysis of the carbon isotope record from the Archean to Phanerozoic and implications for the rise of oxygen. *American Journal of Science* **315**, 275–316.

Laws E. A., Bidigare R. R. and Popp B. N. (1997) Effect of growth rate and CO2 concentration on carbon isotopic fractionation by the marine diatom Phaeodactylum tricornutum. *Limnology and Oceanography* **42**, 1552–1560.

Laws E. A., Popp B. N., Bidigare R. R., Kennicutt M. C. and Macko S. A. (1995) Dependence of phytoplankton carbon isotopic composition on growth rate and $[CO_2]_{aq}$: Theoretical considerations and experimental results. *Geochimica et Cosmochimica Acta* **59**, 1131–1138.

Lyons T. W., Reinhard C. T. and Planavsky N. J. (2014) The rise of oxygen in Earth's early ocean and atmosphere. *Nature* **506**, 307.

Martin W. and Kowallik K. V (1999) Annotated English translation of Mereschkowsky's 1905 paper "Über Natur und Ursprung der Chromatophoren im Pflanzenreiche." *European Journal of Phycology* **34**, 287–295.

Mojzsis S. J., Arrhenius G., McKeegan K. D., Harrison T. M., Nutman A. P. and Friend C. R. L. (1996) Evidence for life on Earth before 3,800 million years ago. *Nature* **384**, 55–59.

Moreira D., Tavera R., Benzerara K., Skouri-Panet F., Couradeau E., Gérard E., Fonta C. L., Novelo E., Zivanovic Y. and López-García P. (2017) Description of Gloeomargarita lithophora gen. nov., sp. nov., a thylakoid-bearing, basal-branching cyanobacterium with intracellular carbonates, and proposal for Gloeomargaritales ord. nov. *International Journal of Systematic and Evolutionary Microbiology* **67**, 653–658.

Parfrey L. W., Lahr D. J. G., Knoll A. H. and Katz L. A. (2011) Estimating the timing of early eukaryotic diversification with multigene molecular clocks. *Proceedings of the National Academy of Sciences* **108**, 13624–13629.

Ponce-Toledo R. I., Deschamps P., López-García P., Zivanovic Y., Benzerara K. and Moreira D. (2017) An Early-Branching Freshwater Cyanobacterium at the Origin of Plastids. *Current Biology* **27**, 386–391.

Popp B. N., Laws E. A., Bidigare R. R., Dore J. E., Hanson K. L. and Wakeham S. G. (1998) Effect of Phytoplankton Cell Geometry on Carbon Isotopic Fractionation. *Geochimica et Cosmochimica Acta* **62**, 69–77.

Price G. D. and Badger M. R. (2003) CO2 concentrating mechanisms in cyanobacteria: molecular components, their diversity and evolution. *Journal of Experimental Botany* **54**, 609–622.

Rae B. D., Long B. M., Badger M. R. and Price G. D. (2013) Functions, Compositions, and Evolution of the Two Types of Carboxysomes: Polyhedral Microcompartments That Facilitate CO_2 Fixation in Cyanobacteria and Some Proteobacteria. *Microbiol. Mol. Biol. Rev.* **77**, 357.

Rasmussen B., Bekker A. and Fletcher I. R. (2013) Correlation of Paleoproterozoic glaciations based on U–Pb zircon ages for tuff beds in the Transvaal and Huronian Supergroups. *Earth and Planetary Science Letters* **382**, 173–180.

Rau G. H., Riebesell U. and Wolf-Gladrow D. (1997) CO2aq-dependent photosynthetic 13C fractionation in the ocean: A model versus measurements. *Global Biogeochemical Cycles* **11**, 267–278.

Raven J. A., Beardall J. and Sánchez-Baracaldo P. (2017) The possible evolution and future of CO2-concentrating mechanisms. *Journal of Experimental Botany* **68**, 3701–3716.

Raven John A., Giordano Mario, Beardall John and Maberly Stephen C. (2012) Algal evolution in relation to atmospheric CO2: carboxylases, carbon-concentrating mechanisms and carbon oxidation cycles. *Philosophical Transactions of the Royal Society B: Biological Sciences* **367**, 493–507.

Sánchez-Baracaldo P., Raven J. A., Pisani D. and Knoll A. H. (2017a) Early photosynthetic eukaryotes inhabited low-salinity habitats. *Proc Natl Acad Sci USA* **114**, E7737.

Sánchez-Baracaldo P., Raven J. A., Pisani D. and Knoll A. H. (2017b) Early photosynthetic eukaryotes inhabited low-salinity habitats. *Proc Natl Acad Sci USA* **114**, E7737.

Schidlowski M., Gorzawski H. and Dor I. (1994) Carbon isotope variations in a solar pond microbial mat: Role of environmental gradients as steering variables. *Geochimica et Cosmochimica Acta* **58**, 2289–2298.

Shih P. M., Hemp J., Ward L. M., Matzke N. J. and Fischer W. W. (2017) Crown group Oxyphotobacteria postdate the rise of oxygen. *Geobiology* **15**, 19–29.

Shih P. M. and Matzke N. J. (2013) Primary endosymbiosis events date to the later Proterozoic with cross-calibrated phylogenetic dating of duplicated ATPase proteins. *Proceedings of the National Academy of Sciences* **110**, 12355–12360.

Ward L. M., Kirschvink J. L. and Fischer W. W. (2016) Timescales of Oxygenation Following the Evolution of Oxygenic Photosynthesis. *Origins of Life and Evolution of Biospheres* **46**, 51–65.

Yoon H. S., Hackett J. D., Ciniglia C., Pinto G. and Bhattacharya D. (2004) A Molecular Timeline for the Origin of Photosynthetic Eukaryotes. *Molecular Biology and Evolution* **21**, 809–818.

Zeebe R. E. and Wolf-Gladrow D. (2001) *CO2 in seawater: equilibrium, kinetics, isotopes*. 1st ed.,

Appendices

Appendix A: The Liquid BG-11 medium recipe for 1L.

100X BG-FPC		**1 L**
FW 84.99	$NaNO_3$	149.58 g
FW 246.47	$MgSO_4$, $7H_2O$	7.49 g
FW 147.02	$CaCl_2$, $2H_2O$	3.6 g
FW 192.13	Citric Acid	.596 g
FW 372.24	Na-EDTA, 119 mM, pH 8.0	2.35 mL
	Trace Minerals	100 mL

Dissolve components in a total volume of 1L H_20. Store at 4 C.

Trace Minerals		**1 L**
FW 61.83	H_3BO_3	2.86 g
FW 197.92	$MnCl_2$, $4H_2O$	1.81 g
FW 287.54	$ZnSO_4$, $7H_20$	0.222g
FW 241.96	Na_2MoO_4, $2H_2O$	0.39 g
FW 249.70	$CuSO_4$, $5H_2O$	0.079 g
FW 291.05	$Co(NO_3)_2$, $6H_20$	0.0494 g

Dissolve components in a total volume of 1L H_20. Store at 4 C.
This is a component of 100X BG-FPC.

1000X Fe ammonium citrate stock solution		**50 mL**
(6mg/ml)	Fe ammonium citrate	0.3 g

Dissolve components in a total volume of 50 mL H_20. Store at 4 C in the dark.

1000X Na_2CO_3 stock (189 mM)		**50 ml**
FW 106.00	Na_2CO_3	1 g

Dissolve components in a total volume of 50 mL H_20. Store at 4 C.

1000X K_2HPO_4 Stock (175 mM)		**50 mL**
FW 228.22	K_2HPO_4, $3H_2O$	1.997 g

Dissolve components in a total volume of 50 mL H_20. Store at 4 C.

1M HEPES pH 7.8		**250 mL**

Fill volume to ~850 mL H_2O, add in order:

- BG-FPC Stock (10mL)
- Fe Ammonium Citrate Stock (1mL)
- Na_2CO_3 Stock (1mL)
- K_2HPO_4 Stock (1mL)
- HEPES (10mL)

Fill volume to 1L, autoclave for 20 min, and store at RT in the dark.

Appendix B: The BG-11 medium recipes comparison

Concentration (mM)	**Commercial Version**	**Paris Laboratory**	**Cameron Laboratory**
$NaNO_3$	17.6	17.65	1.00
K_2HPO_4	0.23	0.23	-
K_2HPO_4 $3H_2O$	-	-	0.175
MgSO4 $7H_2O$	0.3	0.30	0.3
$CaCl_2$ $2H_2O$	0.24	0.24	0.24
Citric Acid H_2O	0.031	-	-
Citric Acid Anhydrous	-	0.029	0.31
Ferric Ammonium Citrate	0.021	0.023	0.023
Na_2EDTA $2H_2O$	0.0027	-	0.0028
Na_2CO_3	0.19	-	0.19
$NaHCO_3$	-	0.48	-
Sodium Thiosulfate Pentahydrate	1	-	-
Vitamin B12	-	4 µg/L	-
INDRIAL	-	0.0023	-
HEPEs	-	-	10
Trace Metals	1ml/L	1ml/L	1ml/L
• H_3BO_3	-	0.0463	0.0463
• $MnCl_2$ $4H_2O$	-	0.0091	0.0091
• $ZnSO_4$ $7H_2O$	-	0.00077	0.00077
• Na_2MoO_4 $7H_2O$	-	0.0016	0.0016
• $CuSO_4$ $5H_2O$	-	0.00032	0.00032
• $Co(NO_3)_2$ $6H_2O$	-	0.00017	0.00017

Appendix C: The result from calculation for dissolved carbon dioxide concentration and other species by csys.m function obtained from https://www.soest.hawaii.edu/oceanography/faculty/zeebe_files/CO2_System_in_Seawater/csys.html

Input for csys.m function

Conditions	**Temperature**	**Salinity**	**Total Pressure**	**pH**	**Partial pressure of CO_2**
[Unit]	˚C	*NA*	atm	*NA*	atm
Air	30	0	0.821	7.47	0.0003284
3% CO_2	30	0	0.821	6.91	0.02463

Output for csys.m function

Conditions	$[CO_2]$	$[HCO_3^-]$	$[CO_3^{2-}]$	**DIC**	**Alk**	**pHtotal**	**pHfree**
[Unit]	µmol/kg	µmol/kg	µmol/kg	µmol/kg	µmol/kg	*NA*	*NA*
Air	9.81	246.31	3.08	259.20	252.86	7.47	7.47
3% CO_2	735.55	5087.89	17.53	5840.97	5122.94	6.91	6.91

Appendix D: The net growth rates of cyanobacterial strains as a function of dissolved carbon dioxide levels A) *Synechococcus* sp. PCC 6312, B) *Synechococcus* sp. PCC 7002, C) *Gloeomargarita lithophora* and D) *Neosynechococcus sphagnicola.* Error bars represent standard deviation of growth rate from biological replicates under different CO_2 conditions.